Suppression of antiferromagnetic spin fluctuations in superconducting Cr$_{0.8}$Ru$_{0.2}$

M. Ramazanoglu,[1,2] B. G. Ueland,[3] D. K. Pratt,[4] L. W. Harriger,[4] J. W. Lynn,[4] G. Ehlers,[5] G. E. Granroth,[5] S. L. Bud'ko,[3,6]
P. C. Canfield,[3,6] D. L. Schlagel,[3] A. I. Goldman,[3,6] T. A. Lograsso,[3,7] and R. J. McQueeney[3,6]

[1]*Physics Engineering Department, Istanbul Technical University, 34469, Maslak, Istanbul, Turkey*
[2]*Brockhouse Institute for Materials Research, Hamilton, ON L8S 4M1 Canada*
[3]*Ames Laboratory, Ames, Iowa 50011, USA*
[4]*NIST Center for Neutron Research, National Institute of Standards and Technology, Gaithersburg, Maryland 20899, USA*
[5]*Oak Ridge National Laboratory, Oak Ridge, Tennessee 37831, USA*
[6]*Department of Physics and Astronomy, Iowa State University, Ames, Iowa 50011, USA*
[7]*Department of Materials Science and Engineering, Iowa State University, Ames, Iowa 50011, USA*

Unconventional superconductivity (SC) often develops in magnetic metals on the cusp of static antiferromagnetic (AFM) order where spin fluctuations are strong. This association is so compelling that many SC materials are labeled as unconventional by proximity to an ordered AFM state. The Cr-Ru alloy system possesses such a phase diagram [see Fig. 1(a)]. Here we use inelastic neutron scattering to show that spin fluctuations are present in a SC Cr$_{0.8}$Ru$_{0.2}$ alloy ($T_c = 1.35$ K). However, the neutron spin resonance, a possible signature of unconventional SC, is not observed. Instead, data indicate a spin gap of order 2Δ (the superconducting gap) and a suppression of magnetic spectral weight at energies well above 2Δ. The suppression decreases the magnetic exchange energy, suggesting that low energy spin fluctuations *oppose* the formation of SC. In conjunction with other experimental evidence, a possible scenario is that *conventional* SC sits on the cusp of AFM order in Cr-Ru alloys.

I. INTRODUCTION

Body-centered cubic (BCC) Cr metal is the prototypical itinerant AFM where spin-density wave (SDW) ordering occurs due to nesting of electron and hole pockets on the Fermi surface [Fig. 1(b)] [1]. Alloying Cr with Ru or Re suppresses SDW order and stabilizes SC [Fig. 1(a)] [2–5], a phenomenon which is similar to the appearance of unconventional SC in the cuprates, iron pnictides, and heavy fermion-based SC [6]. The proximity of AF ordering and SC suggests that Cr alloys, with their BCC structure and weak electron-electron interactions, may be the simplest manifestation of unconventional SC that nature has to offer, and this confirmation would be an important milestone in condensed matter physics.

A key signature of unconventional SC is that the SC gap (or pair wave function) changes sign on the Fermi surface. Cuprates and heavy fermion SC adopt an unconventional *d*-wave gap, possessing gapless points (nodes) that can be inferred from heat capacity, penetration depth, and spectroscopic methods. Alternately, the sign of the gap may be observed directly via phase-sensitive tunnel junction methods [7]. In Cr-Ru alloys, heat capacity measurements [Fig. 1(c)] can be understood from weak-coupling BCS theory with an isotropic *s*-wave electronic gap [5], consistent with conventional electron-phonon driven SC. The jump in the heat capacity at T_c ($\Delta/T_c \approx 10$ mJ mol^{-1} K^{-1}) [8] and the ratio of T_c and the Fermi temperature ($T_c/T_F \approx 10^{-4}$) [9] are also consistent with conventional SC found in other elemental SCs. However, this does not exclude Cr-Ru from being an unconventional SC. Similar to iron pnictides, the nested electron and hole pockets can support an unconventional SC gap without any nodes, but with an opposite sign on different Fermi surface

pockets (a so-called s_{+-} gap) [10]. Differentiating between unconventional s_{+-} and conventional s_{++} gaps [11] is much more difficult experimentally due to the absence of nodes and the difficulty of employing phase sensitive methods [12].

In this regard, inelastic neutron scattering (INS) is a powerful method to test for the presence of unconventional SC. The observation of a gap-peak feature in the spin fluctuation spectrum, called the neutron spin resonance, arises from enhancements due to a "sign-changing" unconventional SC gap. Observations of the spin resonance have confirmed the existence of *d*-wave SC in cuprates [7] and heavy fermion SC [13]. More importantly, observation of the resonance provides an essential experimental verification of multiband s_{+-} gaps found in iron pnictides. For a conventional s_{++} gap, INS would observe a gap at 2Δ and weak enhancement of spin fluctuations above the gap [14].

We have performed INS studies on a Cr$_{0.8}$Ru$_{0.2}$ alloy with $T_c = 1.35$ K. We find that energetic and sharply defined spin fluctuations are present [Fig. 1(d)]. Their large energy scale (>150 meV) is similar to that found for the SDW ordered Cr metal [1] and other Cr alloys [16,17] and not unlike those observed in iron pnictide [14] and cuprate SC [18]. However, we are unable to ascertain the existence of a neutron spin resonance below the SC gap ($2\Delta \approx 3.5k_B T_c \approx 0.5$ meV) due to a vanishingly small normal state magnetic spectral weight of <0.001 μ_B at these energies. This means that we cannot make a definite conclusion about the existence of a spin resonance. However, we do observe the development of a spin gap of order 2Δ and an overall suppression of the spin fluctuations up to 6 meV in the SC state. While not an absolute test of the pairing mechanism, the loss of low energy magnetic spectral weight in the SC state and the corresponding loss of
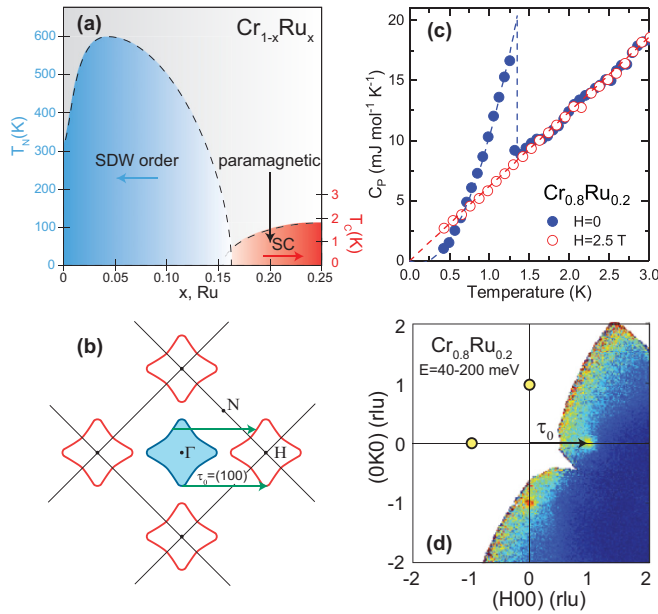
FIG. 1. (a) Schematic phase diagram for $Cr_{1-x}Ru_x$ alloy showing SDW ordered, paramagnetic, and superconducting (SC) phases (adapted from Ref. [5]). (b) Schematic diagram of Fermi surfaces in the $(HK0)$ plane. Electron pockets at Γ (000) and symmetry-related hole pockets at H (100) are connected by the commensurate nesting vector $\boldsymbol{\tau}_0 = (1, 0, 0)$. (c) Heat capacity of $Cr_{0.8}Ru_{0.2}$ at zero field, showing the superconducting transition at $T_C = 1.35$ K and normal state data at $H = 2.5$ T. The dashed lines are fits to the heat capacity data, as described in the Supplemental Material [15]. (d) Inelastic neutron scattering data taken on SEQUOIA in the normal state of $Cr_{0.8}Ru_{0.2}$ showing sharp spin fluctuations at $\boldsymbol{\tau}_0$. Data were measured in the $(HK0)$ plane after averaging over an energy range from 40–200 meV.

AFM exchange energy is consistent with pair breaking spin fluctuations in a conventional s_{++} SC.

II. EXPERIMENTAL DETAILS

Cr metal has incommensurate SDW order with a propagation vector $\boldsymbol{\tau} = \boldsymbol{\tau}_0 + (\delta, 0, 0) = (1 + \delta, 0, 0)$ close to the nesting condition between electron and hole Fermi pockets. Alloys of Cr with V, Mo, Ru, and Re add electrons which modify the nesting and stabilize commensurate SDW order at $\boldsymbol{\tau}_0 = (1, 0, 0)$ [19]. In $Cr_{1-x}Ru_x$, alloying with Ru initially stabilizes commensurate SDW order, but SDW order is suppressed with further substitution, becoming completely suppressed above $x_c = 0.17$. Beyond x_c, SC appears with T_c up to at least 2 K, as shown in Fig. 1(a) [2,4,5]. A 40 gram single-crystal sample of $Cr_{0.8}Ru_{0.2}$ was grown by the arc zoning method [20] (see the Supplemental Material (SM) for more information [15]). The crystal mosaic of the sample is less than 0.6 degrees and no long-range magnetic order was detected by neutron diffraction. Heat capacity measurements were performed using the dilution refrigerator option of a Quantum Design physical property measurement system and the semiadiabatic heat pulse technique. Our $Cr_{0.8}Ru_{0.2}$ sample has $T_c = 1.35$ K [as determined from the onset of sharp peak in the heat capacity, as shown in Fig. 1(c)].

INS measurements were performed on the SEQUOIA [21] and CNCS neutron chopper spectrometers at the Spallation Neutron Source at Oak Ridge National Laboratory and the BT-7 [22] and SPINS triple-axis spectrometers at the NIST Center for Neutron Research. Details of the instrument configurations can be found in the SM [15]. For CNCS and SEQUOIA, the crystal was mounted with a $(HK0)$ horizontal scattering plane with measurements performed on series of rotations around the c axis of the crystal to sweep out the full four-dimensional scattering function.

INS can determine the momentum ($\boldsymbol{Q}$) and energy (E) dependence of the spin fluctuations. The neutron intensity, $S(\boldsymbol{Q}, E)$, is proportional to the imaginary part of the dynamical magnetic susceptibility, $\chi''(\boldsymbol{Q}, E)$,

$$S(\boldsymbol{Q}, E) = f^2(\boldsymbol{Q})e^{-2W}\frac{(\gamma r_0)^2}{2\pi \mu_B^2}[1 + n(E)]\chi''(\boldsymbol{Q}, E). \quad (1)$$

$\boldsymbol{Q} = \frac{2\pi}{a}(H, K, L)$ is defined in reciprocal lattice units (rlu) where $a = 2.91$ Å. $\chi''(\boldsymbol{Q}, E) = \chi''_{zz}(\boldsymbol{Q}, E)$ corresponds to the isotropic susceptibility appropriate for a cubic system, $n(E)$ is the Bose occupancy factor, $f(\boldsymbol{Q})$ is the magnetic form factor for Cr metal [23], e^{-2W} is the Debye-Waller factor, and $(\gamma r_0)^2 = 290.6$ mb sr^{-1} relates the magnetic moment to the neutron cross section. The isotropic susceptibility is extracted in units of μ_B^2 eV^{-1} atom^{-1} by calibration to a phonon of known cross section (see SM [15]).

III. RESULTS

We determined the normal state spin fluctuations of $Cr_{0.8}Ru_{0.2}$ measured above T_c. Cuts through the magnetic spectrum in Figs. 1(d) and 2(a)–2(e) indicate that spin fluctuations are commensurate at all energies and centered at $\boldsymbol{\tau}_0 = (1, 0, 0)$. Figure 2 shows that spin fluctuations persist up to at least 150 meV. This energy scale is analogous to Cr metal [1,16] and Cr-V alloys [17] where high energy spin excitations emanate from incommensurate ($\boldsymbol{\tau}$) and commensurate wave vectors ($\boldsymbol{\tau}_0$), respectively, and are observed up to 400 meV. Similarities can also be drawn to the steep magnetic excitations observed in iron pnictide [14] and cuprate superconductors [18].

The normal state paramagnetic spectrum is modeled using a spherical Gaussian form, consistent with previous investigations of Cr and its alloys [17,24],

$$\chi''(\boldsymbol{Q}, E) = \chi''(\boldsymbol{\tau}_0, E)e^{-|\boldsymbol{Q}-\boldsymbol{\tau}_0|^2/2\kappa^2}, \quad (2)$$

where κ is the momentum-space peak width in rlu. Fits to reciprocal space cuts at fixed E [Fig. 2(e)] allow the determination of the local dynamical susceptibility by averaging over the Brillouin zone

$$\chi''(E) = \frac{\int_{BZ} \chi''(\boldsymbol{Q}, E)d\boldsymbol{Q}}{\int_{BZ} d\boldsymbol{Q}} = \frac{(2\pi)^{3/2}\kappa^3 \chi''(\boldsymbol{\tau}_0, E)}{V_{BZ}}, \quad (3)$$

where $V_{BZ} = 2$ rlu^3 for a BCC lattice. Figure 2(f) shows the normal state local dynamical susceptibility obtained from several different instruments and configurations. The energy dependence is modeled using a relaxational form typically
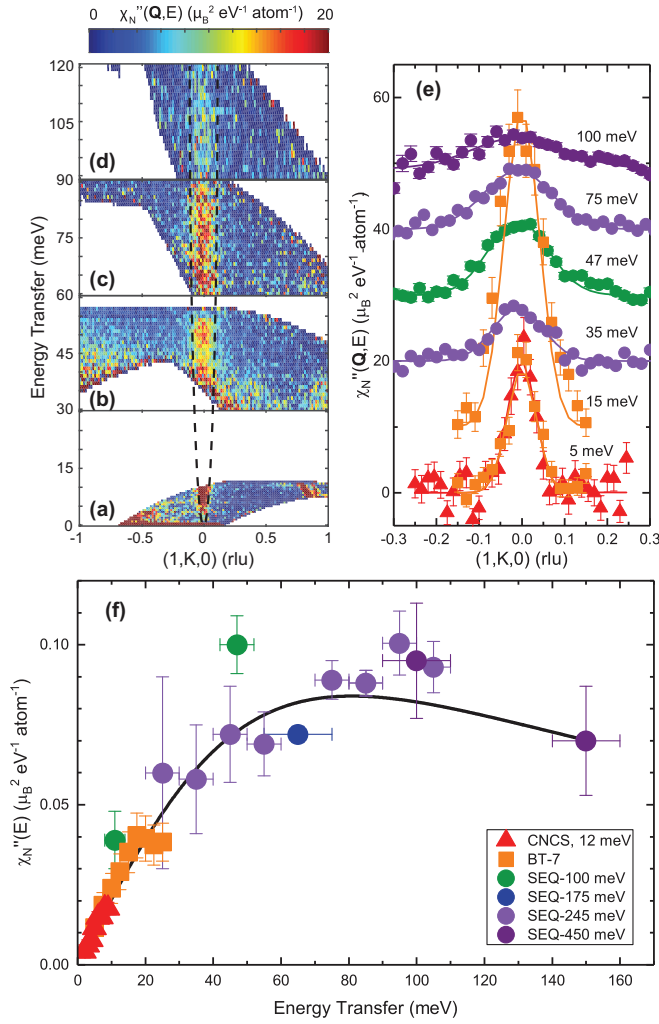
FIG. 2. Steep magnetic excitations centered at $\tau_0 = (1, 0, 0)$ are shown over different energy ranges obtained with the following instrument configurations (a) CNCS-12 meV, (b) SEQUOIA-100 meV, (c) SEQUOIA-245 meV, and (d) SEQUOIA-450 meV. The background was estimated from nearby cuts and subtracted. For (a), the data have been averaged from $H = 0.95$ to 1.05 rlu and $L = -0.05$ to 0.05 rlu. For (b)–(d), the data have been averaged from $H = 0.9$ to 1.1 and $L = -0.1$ to 0.1 rlu. (e) Transverse cuts through τ_0 averaged over different energy bands using the instrument configurations indicated in the legend of panel (f). Lines correspond to fits to Eq. (2). (f) The local susceptibility obtained from the average of the magnetic spectral weight over the entire Brillouin zone. The line is a fit to the relaxational form [Eq. (4)]. For all plots, the dynamical susceptibility is normalized in absolute units of μ_B^2 eV^{-1} atom^{-1} by comparison to a reference phonon. CNCS and BT-7 data were measured at 2.6 K and SEQUOIA data at 5 K.

used for paramagnetic metals,

$$\chi''(E) = \chi_0 E\Gamma/(E^2 + \Gamma^2), \qquad (4)$$

where Γ is the spin fluctuation energy scale and χ_0 is the staggered susceptibility. A fit of $\chi''(E)$ to this function is shown in Fig. 2(f) and gives $\Gamma = 81(5)$ meV, similar to Cr-V alloys, and $\chi_0 = 0.17(1)\mu_B^2$ eV^{-1} atom^{-1}.
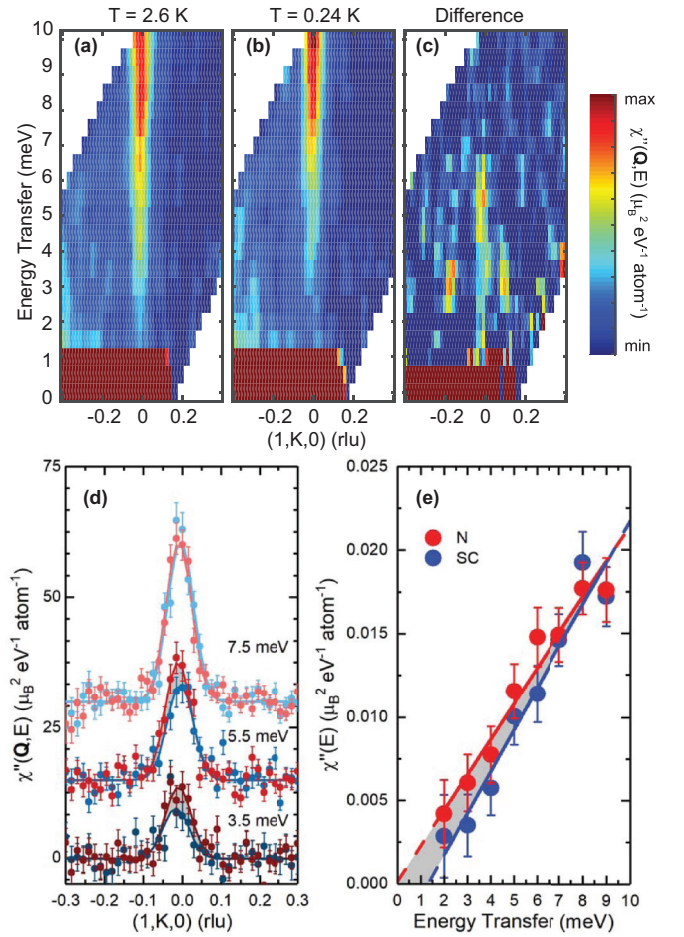
FIG. 3. Spin fluctuations in (a) the normal state at $T=2.6$ K, (b) in the SC state at $T=0.24$ K, and (c) the difference of normal minus SC intensity. For (a) and (b) the min and max intensity levels on the color bar are 0 and 40. For (c), the min and max levels are 0 and 10. (d) Reciprocal space cuts through the data at several energy transfers in the normal state (red dots) and the SC state (blue dots). The shaded area highlights the suppression of the intensity in the SC state. (e) The local susceptibility obtained from Eq. (3) in the normal (red dots) and SC (blue dots) states. Lines are linear fits to the susceptibility as described in the text. In (a)–(d), a background has been estimated and subtracted from the data (see SM [15]).

The fluctuating moment is determined up to a cutoff energy E_c by the sum rule

$$\langle m^2 \rangle = \frac{3}{\pi} \int_{-E_c}^{E_c} \chi''(E)[1 + n(E)]dE. \qquad (5)$$

Assuming that Eq. (4) holds up to $E_c = 300$ meV, the fluctuating moment in the paramagnetic state of $Cr_{0.8}Ru_{0.2}$ is $\sqrt{\langle m^2 \rangle} \approx 0.15 \, \mu_B$ atom^{-1}, comparable to the ordered moment of Cr metal ($\approx 0.6 \, \mu_B$) [1].

We focus on low energies to ascertain the influence of SC on the spin fluctuations. For most unconventional SC, the spin resonance and other modifications to the spin fluctuation spectrum occur in a range of energies up to 3–$5 \, k_B T_c$ and are visible deep within the SC state [25]. For $T_c = 1.35$ K, this requires measurements be performed below 1 meV at temperatures well below 1 K. We carried out cold neutron

measurements in the normal ($T = 2.6$ K) and SC ($T = 0.24$ K) states on CNCS in two configurations, $E_i = 3.65$ meV and 12 meV, with energy resolution HWHM of 0.05 and 0.20 meV, respectively.

Figure 3 shows a comparison of the normal and SC magnetic spectra above and below T_c over an energy range from $E = 0$–10 meV, including comparisons of the Q-dependent and local susceptibilities. Unfortunately, we cannot detect any magnetic signal below 1.5 meV in either state due to its inherent weakness and signal-to-background limitations (see SM for details [15]). This weakness can be quantified by using Eq. (4), which is linear at low energies ($E \ll \Gamma$). The normal state fluctuating moment can be estimated at $T = 0$ and up to $2\Delta \approx 0.5$ meV using Eq. (5)

$$\langle m^2 \rangle_{\text{SC}} \approx \frac{3}{\pi} \int_0^{2\Delta} \chi''(E)\,dE \approx \frac{6\Delta^2}{\pi}\frac{\chi_0}{\Gamma}, \qquad (6)$$

where $\chi_0/\Gamma = 2.1(2)$ μ_B^2 eV^{-2} atom^{-1}. We obtain a vanishingly small fluctuating moment of $\sqrt{\langle m^2 \rangle_{\text{SC}}} \approx 5.0(4) \times 10^{-4}$ μ_B at energies below 2Δ, which is too small to directly test for the presence of a spin resonance or a spin gap.

On the other hand, Fig. 3(e) demonstrates that the SC transition suppresses the dynamical susceptibility up to $E \approx 6$ meV, and linear fits to the local susceptibility in the SC state are consistent with a spin gap of $E_g = 1.3 \pm 0.6$ meV, which is of order 2Δ. The simplest interpretation of the suppression of spectral weight above 2Δ is a reduction in the fluctuating moment below T_c, presumably due to the opening of the SC gap. Comparable behavior is found in the loss of the static magnetic moment in the SC state of the iron pnictides where long-range AFM order coexists with and competes with SC [26].

IV. ESTIMATE OF THE MAGNETIC EXCHANGE ENERGY

The loss of moment ($\delta\langle m^2 \rangle$) in the SC state results in a decrease of magnetic exchange energy (δF_{ex}), which can be estimated at $T = 0$ from the local susceptibility [27,28]

$$\delta F_{ex} = \frac{-3J_{\text{eff}}}{\pi(g\mu_B)^2} \int [\chi_N''(E) - \chi_S''(E)]\,dE = \frac{-J_{\text{eff}}\delta\langle m^2 \rangle}{(g\mu_B)^2}, \qquad (7)$$

where the effective magnetic exchange $J_{\text{eff}} \gtrsim 100$ meV can be estimated from the spin wave velocity (see SM [15]) and $g \approx 2$. Based on the linear fits in Fig. 3(e), we obtain $\delta F_{ex} \approx -4(4) \times 10^{-4}$ meV atom^{-1} where the negative sign indicates that the spin fluctuations *oppose* superconductivity. This can be compared to the SC condensation energy obtained from the heat capacity data in Fig. 1(c), $\delta F_{\text{SC}} = 2.7(9) \times 10^{-5}$ meV atom^{-1}. A comparison of these numbers ($\frac{\delta F_{ex}}{\delta F_{\text{SC}}} \approx -10$) indicates that low energy spin fluctuations have a strongly negative influence on SC (see SM for details [15]).

In other unconventional SC where this quantity has been measured [13,29], the large resonant enhancement of the low energy spectral weight, $\frac{\delta F_{ex}}{\delta F_{\text{SC}}} \approx +10$, strongly supports a magnetic mechanism for pairing within the theory outlined in Refs. [27,28]. To support a magnetic mechanism for Cr-Ru, application of this theory would require a large resonant enhancement of $\frac{3}{\pi}\int \chi_{\text{res}}''(E)\,dE \sim 2\delta\langle m^2 \rangle = 3 \times 10^{-5}$ μ_B^2 atom^{-1} sufficient to overcome the high-energy
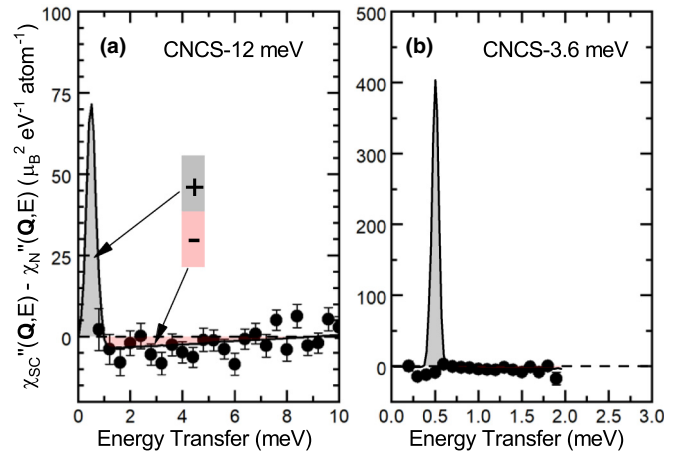
FIG. 4. Simulated intensity of the enhanced neutron spectral weight at $E = 2\Delta$ (gray shaded peak) that is required to overcome the negative spectral weight (pink shaded area) for two configurations (a) CNCS-12 meV and (b) CNCS-3.65 meV. The data points are obtained by subtracting the normal state data at 2.6 K from the SC data at 0.24 K after averaging over a (H, K, L) box centered at τ_0 of size ± 0.05 rlu in all directions.

suppression. Assuming a resolution-limited resonance in Q and E and positioned at $E = 2\Delta$, we can model the cross section to test for observability, as shown in Fig. 4. Our simulations indicate that a spin resonance of this size should be observable under our experimental conditions, and we therefore conclude that no resonant enhancement exists with sufficient size to overcome the observed loss of exchange energy. This conclusion is also supported by data taken on SPINS, as shown in the SM [15].

V. SUMMARY

We summarize these interesting results with two possible scenarios. The first scenario assumes that Cr-Ru is an unconventional SC. Here, our observations of disparate SC and spin fluctuation energy scales ($2\Delta/\Gamma \approx 0.01$) [30], small fluctuating moment, and the 3D BCC structure [31] would act to severely reduce the spectral weight of the spin resonance. Thus, we cannot conclude that Cr-Ru is a conventional SC based on the lack of a spin resonance, which may be too weak to observe. Also, other known unconventional SC, such as La$_{2-x}$Sr$_x$CuO$_4$ [32] and HgBa$_2$CuO$_{4+\delta}$ [33], do not display a spin resonance in INS data. The second scenario assumes that Cr-Ru is a conventional SC. In elemental Cr and Cr-Ru alloys with $x < x_c$, SDW order is stabilized by an electronic gap [5,34]. Close to x_c, the reduced SDW gap and SC gap compete for the Fermi surface. In the paramagnetic SC state for $x > x_c$, the remaining low-energy spin fluctuations can be pair-breaking [35], as supported by our estimates of the loss of magnetic exchange and also by the simple fact that T_c increases beyond x_c [5]. Given the experimental evidence and the results presented here, it is plausible that both static SDW order and spin fluctuations act to suppress *conventional* SC. A hardening of the spin fluctuation spectrum in the conventional SC state or a feedback mechanism for which the opening of a SC gap reduces the size of the fluctuating moment could explain the suppression of magnetic spectral weight.

[1] E. Fawcett, Rev. Mod. Phys. **60**, 209 (1988).

[2] B. T. Matthias, T. H. Geballe, V. B. Compton, E. Corenzwit, and G. W. Hull, Jr., Phys. Rev. **128**, 588 (1962).

[3] Y. Nishihara, Y. Yamaguchi, T. Kohara, and M. Tokumoto, Phys. Rev. B **31**, 5775 (1985).

[4] Y. Nishihara, Y. Yamaguchi, M. Tokumoto, K. Takeda, and K. Fukamichi, Phys. Rev. B **34**, 3446 (1986).

[5] K. Chatani and Y. Endoh, J. Phys. Soc. Jpn. **72**, 17 (2003).

[6] G. R. Stewart, Adv. Phys. **66**, 75 (2017).

[7] M. Eschrig, Adv. Phys. **55**, 47 (2006).

[8] J. S. Kim, G. R. Stewart, S. Kasahara, T. Shibauchi, T. Terashima, and Y. Matsuda, J. Phys.: Condens. Matter **23**, 222201 (2011).

[9] Y. Cao, V. Fatemi, S. Fang, K. Watanabe, T. Taniguchi, E. Kaxiras, and P. Jarillo-Herrero, Nature (London) **556**, 43 (2018).

[10] I. I. Mazin, D. J. Singh, M. D. Johannes, and M. H. Du, Phys. Rev. Lett. **101**, 057003 (2008).

[11] S. Onari, H. Kontani, and M. Sato, Phys. Rev. B **81**, 060504 (2010).

[12] P. J. Hirschfeld, M. M. Korshunov, and I. I. Mazin, Rep. Prog. Phys. **74**, 124508 (2011).

[13] C. Stock, C. Broholm, J. Hudis, H. J. Kang, and C. Petrovic, Phys. Rev. Lett. **100**, 087001 (2008).

[14] P. Dai, Rev. Mod. Phys. **87**, 855 (2015).

[15] See Supplemental Material at http://link.aps.org/supplemental/10.1103/PhysRevB.98.134512 for details.

[16] O. Stockert, S. M. Hayden, T. G. Perring, and G. Aeppli, Phys. B: Condens. Matter **281-282**, 701 (2000).

[17] S. M. Hayden, R. Doubble, G. Aeppli, T. G. Perring, E. Fawcett, J. Lowden, and P. W. Mitchell, Physica B: Condens. Matter **237-238**, 421 (1997).

[18] R. Coldea, S. M. Hayden, G. Aeppli, T. G. Perring, C. D. Frost, T. E. Mason, S. W. Cheong, and Z. Fisk, Phys. Rev. Lett. **86**, 5377 (2001).

[19] E. Fawcett, H. L. Alberts, V. Y. Galkin, D. R. Noakes, and J. V. Yakhmi, Rev. Mod. Phys. **66**, 25 (1994).

[20] T. A. Lograsso and F. A. Schmidt, J. Cryst. Growth **110**, 363 (1991).

[21] G. E. Granroth, A. I. Kolesnikov, T. E. Sherline, J. P. Clancy, K. A. Ross, J. P. C. Ruff, B. D. Gaulin, and S. E. Nagler, J. Phys: Conf. Ser. **251**, 012058 (2010).

[22] J. W. Lynn, Y. Chen, S. Chang, Y. Zhao, S. Chi, W. Ratcliff II, B. G. Ueland, and R. W. Erwin, J. Res. NIST **117**, 61 (2012).

[23] R. M. Moon, W. C. Koehler, and A. L. Trego, J. Appl. Phys. **37**, 1036 (1966).

[24] B. H. Grier, G. Shirane, and S. A. Werner, Phys. Rev. B **31**, 2892 (1985).

[25] G. Yu, Y. Li, E. M. Motoyama, and M. Greven, Nat. Phys. **5**, 873 (2009).

[26] D. K. Pratt, W. Tian, A. Kreyssig, J. L. Zarestky, S. Nandi, N. Ni, S. L. Bud'ko, P. C. Canfield, A. I. Goldman, and R. J. McQueeney, Phys. Rev. Lett. **103**, 087001 (2009).

[27] D. J. Scalapino and S. R. White, Phys. Rev. B **58**, 8222 (1998).

[28] E. Demler and S.-C. Zhang, Nature (London) **396**, 733 (1998).

[29] O. Stockert, J. Arndt, E. Faulhaber, C. Geibel, H. S. Jeevan, S. Kirchner, M. Loewenhaupt, K. Schmalzl, W. Schmidt, Q. Si, and F. Steglich, Nat. Phys. **7**, 119 (2011).

[30] A. Abanov and A. V. Chubukov, Phys. Rev. B **62**, R787 (2000).

[31] A. V. Chubukov and L. P. Gor'kov, Phys. Rev. Lett. **101**, 147004 (2008).

[32] H. Jacobsen, I. A. Zaliznyak, A. T. Savici, B. L. Winn, S. Chang, M. Hücker, G. D. Gu, and J. M. Tranquada, Phys. Rev. B **92**, 174525 (2015).

[33] M. K. Chan, C. J. Dorow, L. Mangin-Thro, Y. Tang, Y. Ge, M. J. Veit, G. Yu, X. Zhao, A. D. Christianson, J. T. Park, Y. Sidis, P. Steffens, D. L. Abernathy, P. Bourges, and M. Greven, Nat. Commun. **7**, 10819 (2016).

[34] A. L. Trego and A. R. Mackintosh, Phys. Rev. **166**, 495 (1968).

[35] A. J. Millis, S. Sachdev, and C. M. Varma, Phys. Rev. B **37**, 4975 (1988).